# CAPACITY OF HYBRID REINFORCED UHPC BEAMS IN FLEXURE AND SHEAR

A.Alameer[1], H. Almansour[2] and M. Saatcioglu[3]

1. Graduate Student, Department of Civil Engineering, University of Ottawa, Canada
2. Associate Research Officer, National Research Council Canada, Ottawa, Ontario, Canada
3. Distinguished University Professor & Research Chair, Department of Civil Engineering, University of Ottawa, Ontario, Canada

**Abstract:** Ultra high performance concrete (UHPC) is a modern class of concrete which has been developed based on the need for high resistance to the penetration of corrosion agents like chlorides. Several UHPC prestressed I beams were investigated in the current research project to assess their flexural and shear capacities using nonlinear finite element models. The objective of the research project was to validate the requirements of existing international guidelines for designing UHPC structures. The results of this study showed that the nonlinear finite element models are able to estimate the initiation of first cracking and the propagation of cracks, while predicting stresses in the inelastic range of deformations. More specifically, the nonlinear distribution of stresses in UHPC upon the formation of cracks and their propagation, as well as the contribution of shear reinforcement in controlling shear cracks and affecting shear resisting mechanism are illustrated.

**Keywords**: UHPC, shear, flexure, prestressed

## 1 INTRODUCTION.

## 2 MATERIAL PROPERTES AND MODEL DISCRETIZATIONS.

Ultra-high performance concrete (UHPC) is a new type of concrete developed by selecting particle sizes and gradation in the nono- and micro-scales, targeting the highest possible compaction during placement. The resulting concrete with very high density is called UHPC. UHPC has very low permeability and very high durability compared to traditional normal-strength and high-performance concretes (HPC). The material shows very high compressive strength but with very brittle failure mode. However, the use of fibers as micro reinforcement changes UHPC failure mode to a ductile mode. The material selection and early age curing processes, use of fiber reinforcement, and the stringent quality control employed during production contribute to the high initial cost of UHPC structures. In order to enable mass production and cost effectiveness of the material, performance based design and material optimization become important. Different trials for design and optimization of UHPC structures were conducted first as part of the current investigation. This led to several uncertainties that called for further research and development involving analytical studies. The paper presents the results of this analytical investigation.

Initial efforts for design and optimization involved the use of an existing building code and associated recommended practice. A number of prestressed UHPC I-beams were designed based on the proposed Japanese recommendations (JSCE, 2006). Flexural and shear capacities of these beams were

reassessed subsequently by nonlinear finite element analysis using TNO DIANA. The applicability and validity of the use of existing cracking and post-cracking models developed for traditional concrete were assessed for UHPC. The emphasis was placed on the ability of existing models for estimating shear resistance and the accuracy of such estimates for concrete structures designed using UHPC.

### 2.1 General Characteristics: Geometry and Boundary Conditions

General Characteristics: Geometry and Boundary Conditions The boundary conditions for the beams consisted of simple supports. Two sets of external loads were modeled: (i) a single concentrated load and (ii) two point loads. The first set of loading was intended to study the shear performance of prestressed beams, for which a single load was applied at a distance “a” from the support such that (the shear span to effective depth ratio) a/d exceeds 2 (see Figure 2.1 and 2.2). The second set of loading was to study the flexural performance of prestressed beams where two point loads were applied at one third and two third points on the span. The simple supports used had a hinge on one side and a roller on the other side. The center-to-center span length was 3.00 m. The cross section of the beam consisted of three parts: (i) bottom flange; 150 mm high and 350 mm wide; (ii) web; 280 mm high and 150 mm wide; and (iii) top flange; 120 mm high and 350 mm wide.

The finite element model consisted of two dimensional elements of three types: (i) shell elements to simulate the UHPC (350 mm thicknesses for the flange and 150 mm for the web) (ii) tendon/cable elements to simulate the prestressing tendons; and (iii) frame elements to simulate the shear reinforcement. The model built in the software was used to simulate the bond between reinforcement and UHPC. The bond model was originally developed for traditional reinforced concrete. The discretization followed the concept of uniform element dimensions throughout the beam while sizes of the elements were optimized through a convergence study.

The stress strain relationship for UHPC in the FEM model was based on the Japanese recommendations (JSCE, 2006), as shown in Figure 2.3. This relationship is a conservative simplification of typical test results, often used for design. More precise models that represent the stress strain relationship of observed behavior has not yet been developed. Table 2.1 shows the material properties used in design.

### 2.2 Load Cases for Nonlinear analysis

The loading considered was a monotonically increasing load, well into the inelastic range of deformations. This type of loading enables the study of gradual development of stresses and initiation and development of cracks. Two loads were applied first prior to the application of the monotonic loading; one due to the self-weight and another one representing the effect of prestressing. These two loads remained constant and within the elastic range of deformations. The third load, or the external load, was imposed over 10 steps as monotonically increasing load with intervals of 10% of the maximum failure load. Each step of the load was further divided into sub-steps, the magnitude of which was controlled by a convergence criteria based on the required level of accuracy.

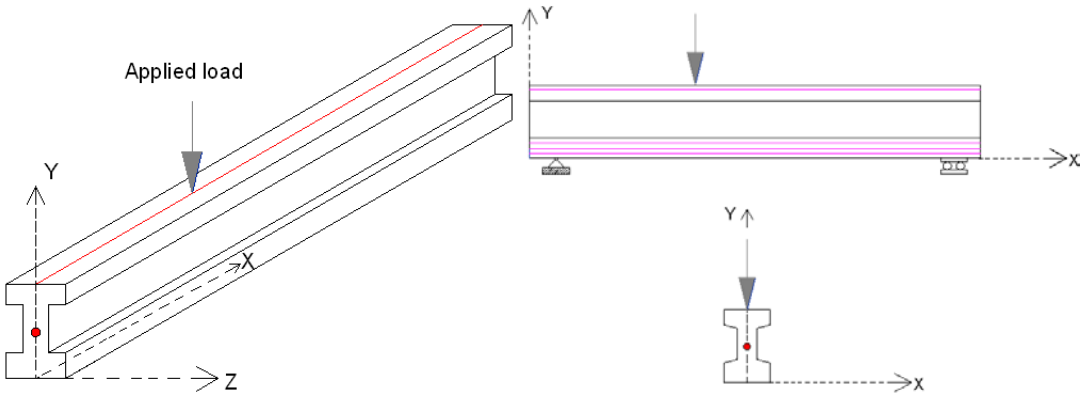


**Figure 2.1 Overview of the prestressed UHPC beam considered under shear loading**

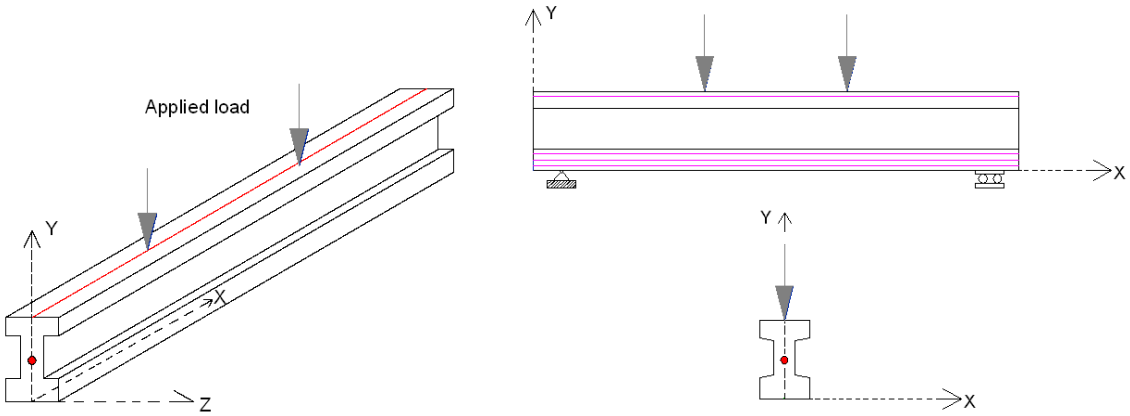


**Figure 2.2 Overview of the prestressed UHPC beam considered for flexural loading**

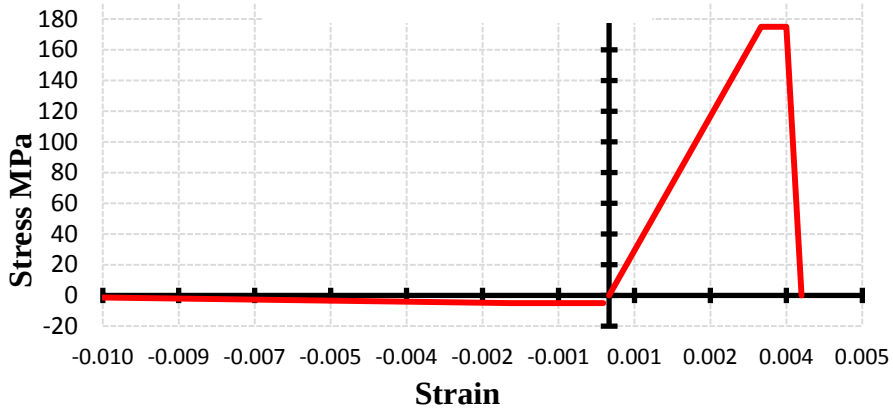


**Figure 2.3 Stress-strain relationship of UHPC**

**Table 2.1 Material properties for design**

| Material | Property | Design Value |
|---|---|---|
| UHPC | Compressive strength ($f'_c$, MPa) | 175 |
| | Tensile Strength ($f_{cr}$, MPa) | 5.3 |
| | Maximum Design Strain in Compression | 0.0035 |
| Tendons (High Strength Steel) | Nominal Strength (MPa) | 1860 |
| | Ultimate design strength (MPa) | 1767 |
| | Pretension Stress (MPa) | 1376 |
| Stirrups (400R Carbon Steel) | Nominal Strength (MPa) | 670 |
| | Yield Stress (MPa) | 430 |

## 3 Results and discussions

Three nonlinear finite elements models are presented in this study for three different UHPC prestressed I-beams. These consisted of a UHPC beam designed for flexural failure, over reinforced for shear (FL1); UHPC beam designed for shear failure with 50 mm stirrup spacing (BS1); and UHPC beam designed for shear failure without stirrups (BS5). These beams were investigated for their load capacity, distribution and flow of stresses, and the mechanism of failure modes.

### 3.1 Load capacity and distribution of stresses

The first model was a UHPC beam designed for flexural failure, which was over-designed in shear, with a stirrups spacing of 50 mm c/c in the two shear zones at both ends (model FL1). The beam geometry and reinforcement arrangement are illustrated in Figure 3.1. The two point loads were applied at one third and two third points of the beam span. These loads were applied on thick steel plates (ASTM A992 Grade 50) with cross sectional dimensions of 100 mm x 100 mm covering the entire width of the beam to avoid stress concentrations at points of loading. Similar steel plates were also used at the supports. Nonlinear finite element analysis was conducted using model FL1 under 10 monotonically-increasing load steps. The distribution of longitudinal stresses at ultimate are presented in Figures 3.2.

The model showed that the ultimate load was 2×2450 kN. Even though the same mechanical properties were considered for the nonlinear FEM and the 2006 JSCE simplified design method, the nonlinear FEM model resulted in higher ultimate load than that given by JSCE. In other words, the 2006 JSCE simplified approach underestimated the UHPC flexural capacity. The maximum compressive stress in this case was 136 MPa or 77.5 % of the UHPC ultimate compressive stress, and the maximum tensile stress in the tendons was 1784 MPa or 96 % of the ultimate strength of steel. On the other hand, the JSCE method resulted in maximum compressive stress of 22 MPa in the critical section (at mid-span) and the stress in the tendons was 1785 MPa. The maximum compressive stress in UHPC is illustrated in Table 3.1, showing that the JSCE approach underestimates the results as computed by FEM analysis. On the other hand, the maximum tensile stress obtained from the 2006 JSCE method and FEM analysis yielded minor differences.

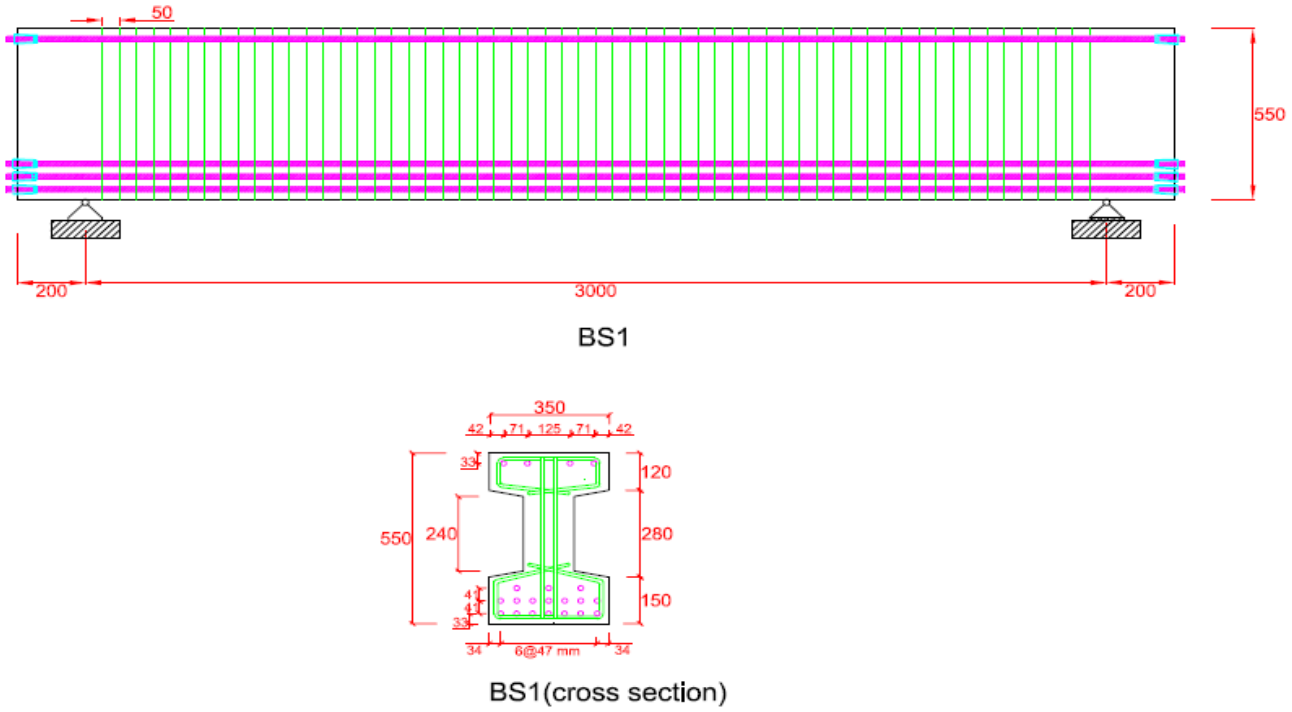


**Figure 3.1 Typical beam details**

**Table 3.1 Summary of stress results from JSCE and FEM analyses**

| Beam type | JSCE, 2006 | | FEM | |
|---|---|---|---|---|
| | Stress at extreme compressive fiber | Stress in tendons | Stress at extreme compressive fiber | Stress in tendons |
| **FL1** | 22.23 | 1785 | 135.6 | 1783.52 |
| **BS1** | 41.99 | 1785 | 118.6 | 1744.3 |
| **BS5** | 12.27 | 1820 | 122.6 | 1763.44 |

The compressive stresses in the beam formed an arch that started from the two supports together with the two points of application of prestressing forces. Table 3.2 shows the comparison between JSCE, 2006 and FEM ultimate loads.

**Table 3.2 Comparisons of applied ultimate loads as computed by JSCE and FEM analysis**

| Model | JSCE, 2006 load (kN) | FEM load (kN) | Difference $\left(\frac{\text{Load}_{\text{JSCE}}-\text{Load}_{\text{FEM}}}{\text{Load}_{\text{JSCE}}}\right) X\ 100$ (%) |
|---|---|---|---|
| **FL1** | 2 X 1656.29 | 2 X 2450 | -47.921 |
| **BS1** | 3018.478 | 3700 | -22.5783 |
| **BS5** | 2095.436 | 3300 | -57.4851 |

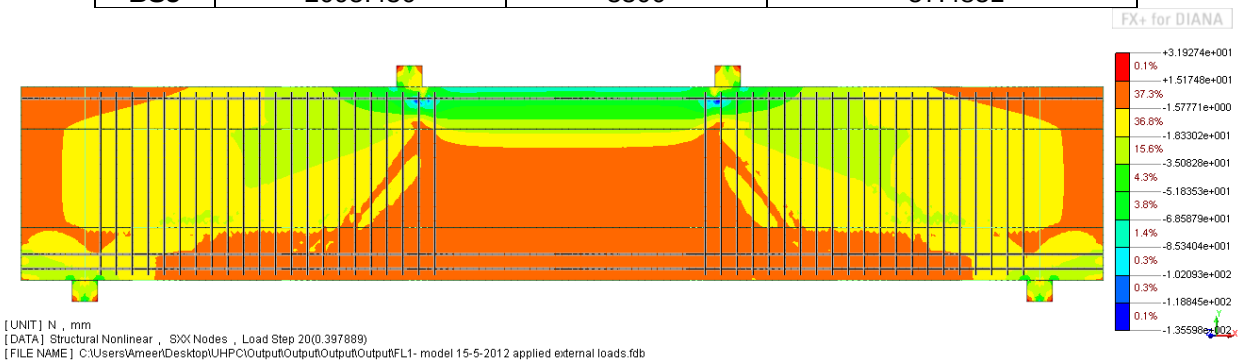


**Figure 3.2 Distribution of longitudinal stresses ($S_{xx}$) in FL1 (Nonlinear model - ultimate load)**

Two additional prestressed UHPC beams, this time designed to fail in shear, i.e., BS1 and BS5, are also presented in this section. Both beams were over-designed for flexure. The objective of this section is to investigate the stress distributions related to different stages of loading, as well as the initiation, formation and progression of cracks in critical loading stages. The loading and support conditions of the beams are illustrated in Figure 3.3 and 3.4. Similar to the beam designed for flexural failure, a single external load was applied on a thick steel plate. Two similarly thick steel plates were used for the beam supports.

The comparisons of analysis results indicate that the ultimate FEM loads for BS1 and BS5 were higher than those computed by using the JSCE approach. The JSCE approach resulted in lower maximum compressive stresses in beam critical sections as seen in Figures 3.3 and 3.4, as well as in Table 3.1. Maximum compressive stresses formed asymmetrical arch, having a maximum stress zone below the applied load. This is shown in Figures 3.3 and 3.4. The diagonal crack that led to the ultimate load condition caused disturbances and fluctuations in stress distributions on both sides of the crack. Table 3.2 shows a summary of stresses computed by the JSCE approach and the FEM analysis.

The maximum compressive stress in BS1 was computed as 119 MPa. The maximum tensile stress in the tendons was 1744 MPa or 94 % of the rupturing strength of steel. The ultimate load that led to this stress state was 3700 KN. In the case of beam BS5, the maximum compressive stress was 138 MPa. The maximum tensile stress in the tendons reached 1666 MPa or 90 % of the ultimate rupturing strength of steel. Also, it was observed that the JSCE method underestimated the applied load and the resultant maximum compressive stress, while the tensile stress had only a minor variation with the results of the FEM analysis.

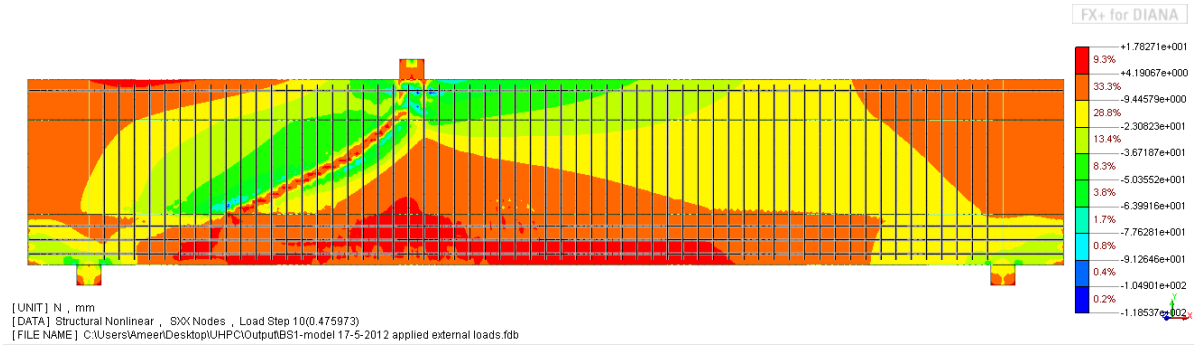


**Figure 3.3 Distribution of longitudinal stresses ($S_{xx}$) in BS1 (Nonlinear model - ultimate load)**

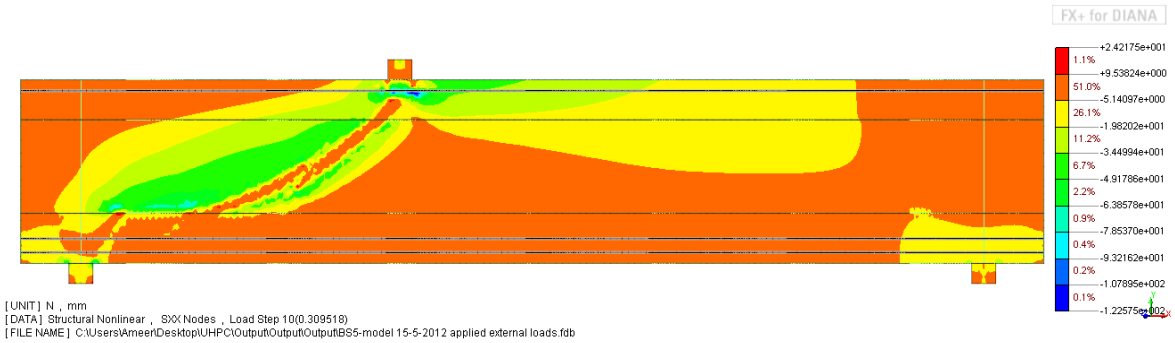


**Figure 3.4 Distribution of longitudinal stresses ($S_{xx}$) in BS5 (Nonlinear model - ultimate load)**

### 3.2 Failure modes and crack pattern

The nonlinear FEM model used is intended for traditional concrete. As such, the effects of fibers and the no-aggregate matrix on the formation and progression of cracks are not considered. FL1 showed a dense distribution of flexural cracks in the bottom flange while major shear cracks were distributed in the web on both sides of the beam. Shear cracks started from the flange-web interface and expanded into diagonal shear cracks.

The widespread distributions of cracks in flexural and shear zones significantly affect the longitudinal stress distribution, and stresses in reinforcement. The failure mode of the flexural model was a mixed shear-flexure failure. The dense propagation of flexural cracks dominated the failure mode. On the other hand, the shear reinforcement controlled shear cracking and prevented compression failure between the cracks within the diagonal crack zone. This is shown in Figure 3.5.

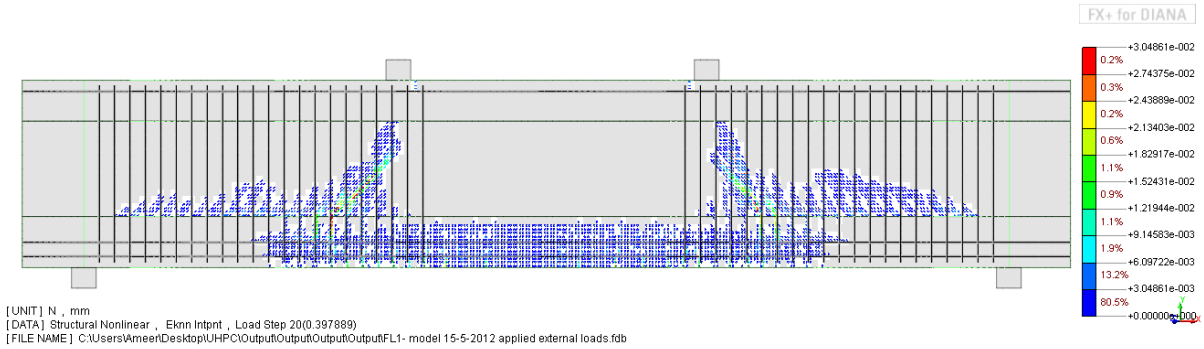


**Figure 3.5 Distribution of cracks in beam FL1 (Nonlinear model - ultimate load)**

The shear model BS1 behaved differently than FL1. A diagonal shear crack was fully formed and bounded by dense shear cracks in the high shear zone (see Figure 3.6). A relatively small shear crack zone developed on the right-hand side of the external load. Heavy flexural cracks localized in a narrow zone below the applied load. The failure occurred when the stress in the tendons reached 95% of the ultimate stress (1744.3 MPa) while the maximum compressive stress was 119 MPa or 68 % of UHPC ultimate compressive stress. This is shown in Figure 3.6.

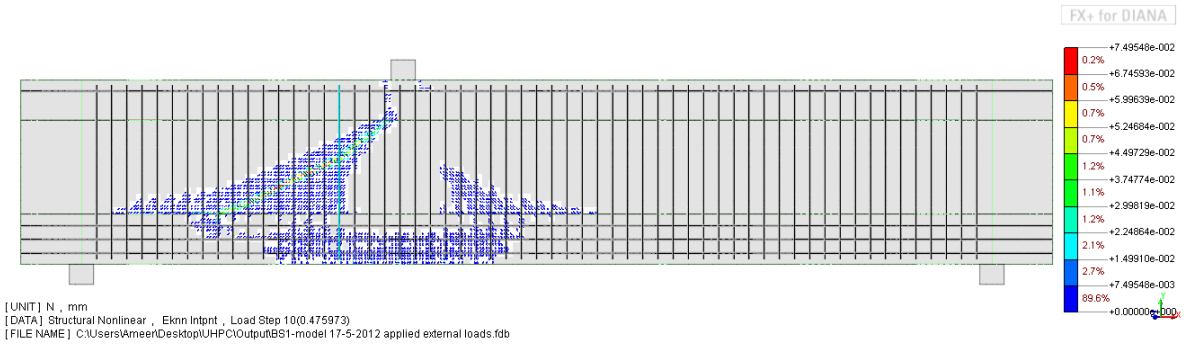


**Figure 3.6 Distribution of cracks in beam BS1 (Nonlinear model – ultimate load)**

Beam (BS5) had no shear reinforcement. The nonlinear finite element model showed that a diagonal shear crack was developed together with a shear crack at the flange-web interface and flexural cracks in the bottom flange under the applied load. The cracks in this case were observed to occur suddenly when the applied load reached 2640 kN. This can be observed in Figure 3.7.

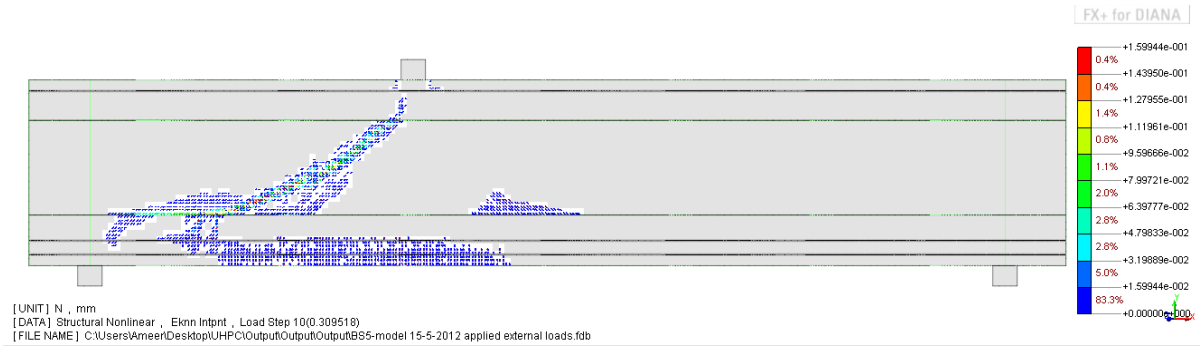


**Figure 3.7 Distribution of cracks in beam BS5 (Nonlinear model – ultimate load)**

After the formation of the diagonal crack there was no clear evidence that the full failure had taken place. Therefore, the applied load was increased to the failure load (3300 kN). The maximum compressive stress in this case was 123 MPa or 70 % of the UHPC ultimate compressive stress. The maximum tensile stress in the tendons was 1763 MPa or 95% of the ultimate stress of steel.

## 4 Conclusions and Future Work

Three UHPC prestressed I-beams were analytically investigated in the current research project. Both FEM analyses and the simplified JSCE approach were used to establish the load capacity, stresses distribution, failure modes, and crack patterns. The results showed that the simplified JSCE approach under-estimated the load capacity. The flexural model showed a mixed shear-flexural failure, and the use of stirrups limited the sudden compression failure. It was concluded that a minimum number of stirrups is required to avoid shear failure.

Non-linear FE models provide promising predictions of flexural and shear behaviour of prestressed UHPC beams. However, these models should be calibrated by a comprehensive experimental study. Further research is needed to develop cracking models for improved analytical predictions. Contrary to earlier recommendations, a minimum amount of stirrup steel was found to be essential to ensure the development of flexural strength. Beyond the minimum stirrup reinforcement needed, the increase in transverse steel (or reduction in stirrup spacing) do not affect the beam behavior.

## 5 References

Almansour, H. and Lounis, Z. “Design of Prestressed UHPFRC Girder Bridges According to Canadian Highway Bridge Design Code”, 2009.

Association Française de Génie Civil (AFGC) “Ultra High Performance Fibre-Reinforced Concretes”, 2002.

Kang, T., Lee, Y., Kim, J., and Kim, Y. “The effect of fiber distribution characteristics on the flexural strength of steel fiber-reinforced ultra-high strength concrete”, 2010.

Japan Society of Civil Engineering, (2006), “Recommendations for Design and Construction of Ultra High Strength Concrete Structures, *Draft*,” *Japanese Society of Civil Engineers, (JSCE),* 2006.

Ma, J. and Schneider, H. “Properties of Ultra-High-Performance Concrete”, 2002.

MacGregor, J. Reinforced concrete: Mechanics and Design, 1992.

Manie, J. “DIANA – Finite Element Analysis User’s Manual release 9.4.4”, TNO DIANA bv, Delft, The Netherlands, 2011.